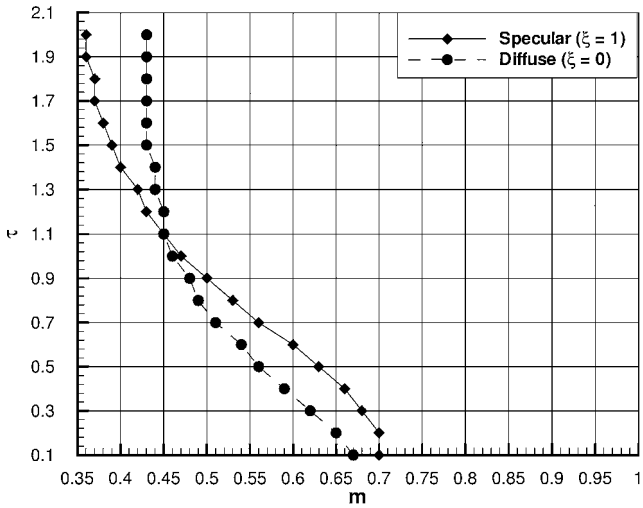

Fig. 4 Minimum-drag power-law coefficients for negligible thermal velocity.

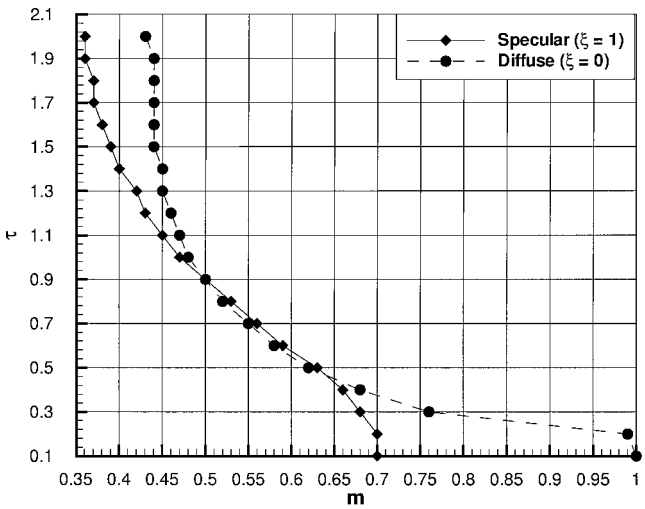

Fig. 5 Minimum-drag power-law coefficients for finite thermal velocity.

curves, as the Carter solution is a subset of this minimum drag power-law solution. These shapes resemble power-law functions with exponents ranging between $\frac{2}{3}$ and $\frac{3}{4}$, quite similar to minimum-drag shapes derived for hypersonic flow under the continuum Newtonian flow assumption of total loss of normal momentum.

Additional calculations were performed with thermal velocity component on the order of one-tenth the spacecraft velocity (which is characteristic for 130-km altitude). Minimum drag coefficients for this condition are shown in Fig. 5. Compared to Fig. 4, the specular curve has essentially no change with the addition of thermal impingement.

Conclusions

Numerical results indicate that the power-law exponent, which corresponds to a minimum-drag body in rarefied flow, is a function of not only the gas-surface interaction model, but the relative magnitude of thermal (that is, random) velocities under realistic orbital conditions. The cases presented include a wide range of practical conditions for an axisymmetric body, although the choice of an optimal shape will obviously depend on the surface material and ambient atmospheric composition. More complicated geometries, including nonaxisymmetric shapes, volume-constrained forms, etc., would have different results and might have to be solved with a completely numerical formulation. In the cases studied, the resulting minimum drag nose geometry under assumption of specular reflection is a weak function of the thermal velocity component. Such a result is to be expected because thermal velocity only influences drag at shallow surface angles, though specular collisions transfer little momentum at shallow angles. In contrast, the exponent for a minimum-drag shape under diffuse reflection was insensitive to the addition of thermal impingement at large τ but significantly affected at $\tau < 0.5$. In this range the optimum nose shape approaches a cone ($m = 1$) because the shallow surface angles receive significant momentum transfer as a result of the thermal velocity. At values of slenderness ratio in the range $0.4 < \tau < 1.0$ with thermal velocity equal to $\frac{1}{10}$ freestream velocity, the mimimum-drag power-law exponent is nearly identical for either specular or diffuse reflection models. This has the very practical benefit that a minimum-drag shape can be selected even though there might be significant uncertainty regarding the nature of gas-surface interactions. The magnitude of drag on that optimal shape will be dependent on the surface interactions.

References

[1]Carter, W. J., "Optimum Nose Shapes for Missiles in the Superaerodynamic Region," *Journal of the Aeronautical Sciences*, Vol. 7, July 1957, pp. 527–532.

[2]Bird, G. A., *Molecular Gas Dynamics and the Direct Simulation of Gas Flows*, Clarendon, New York, 1994, pp. 1–14.

[3]Vincenti, W. G., and Kruger Charles, H. J., *Introduction to Physical Gas Dynamics*, Krieger, Malabar, FL, 1986, pp. 47, 48.

[4]Goodman, F. O., and Wachman, H. Y., *Dynamics of Gas-Surface Scattering*, Academic Press, New York, 1976, pp. 23, 24.

[5]Kuhlthau, A. R., and Bishara, M. N., "On the Nature of the Surface Interaction Between Inert Gas Molecules and Engineering Surfaces," *Rarefied Gas Dynamics*, edited by J. H. de Leeuw, Vol. 2, 1996, pp. 518–535.

[6]Woronowicz, M. S., and Rault, D. F. G., "Cercignani-Lampis-Lord Gas-Surface Interaction Model: Comparisions Between Theory and Simulation," *Journal of Spacecraft and Rockets*, Vol. 31, No. 3, 1994, pp. 532–534.

E. Livne
Associate Editor

Boundary-Layer Instability on Sharp Cone at Mach 3.5 with Controlled Input

T. C. Corke*
University of Notre Dame, Notre Dame, Indiana 46556
D. A. Cavalieri†
Illinois Institute of Technology, Chicago, Illinois 60616
and
E. Matlis‡
University of Notre Dame, Notre Dame, Indiana 46556

Nomenclature

F	=	dimensionless frequency, $2\pi f \nu / U^2$
n	=	oblique wave azimuthal mode number
s	=	azimuthal spacing between actuators
x, y, θ	=	streamwise, wall-normal, and azimuthal directions
λ	=	spanwise wavelength
ψ	=	oblique wave angle

Received 11 January 1999; revision received 4 July 2001; accepted for publication 9 July 2001.

*Clark Professor of Engineering, Center for Flow Physics and Control, Aerospace and Mechanical Engineering Department. Associate Fellow AIAA.

†Graduate Assistant, Mechanical and Aerospace Engineering Department; currently Senior Project Engineer, Bigelow Aerospace, 1899 W. Brooks Avenue, Las Vegas, NV 89032. Member AIAA.

‡Ph.D. Candidate, Center for Flow Physics and Control, Aerospace and Mechanical Engineering Department.

Introduction

A GROWING interest in supersonic flight has brought on a critical need to predict and possibly control transition to turbulence in this flight regime. The challenge for experiments is to control unsteady initial conditions so that direct comparisons can be made to numerical calculations that generally specify initial amplitudes and wave numbers of instability modes leading to transition.

In all of the past experiments, except those of Kosinov et al.,[1] transition to turbulence developed from background disturbances. The problem with that approach is that the character of the freestream disturbances (both vortical and acoustic) are difficult to document completely and are largely facility dependent. In supersonic tunnels with freestream Mach numbers greater than two, disturbances originate from side-wall boundary layers that are unstable and become turbulent. These are felt in the center of the nozzle as acoustic (Mach) waves. The quiet design supersonic nozzles[2] overcome this through a combination of wall suction at the throat and well-designed nozzle expansion sections that have curvature that maximizes the transition Reynolds number for a Goertler instability.

Even if the background disturbances are well documented, a second problem is that the manner by which freestream disturbances enter and excite boundary-layer modes (receptivity) is dependent on the model geometry, such as local curvature, surface junctions, or imperfections (microroughness).

Kosinov et al.[1] aimed at overcoming these problems by introducing periodic disturbances at a point on the surface of a flat plate at $M = 2.0$. The disturbances were produced by a glow discharge between two electrodes in a small cavity below the plate surface. The forcing at a point produced a full spectrum of modes with different wave angles. Ultimately, the most amplified mode was determined by the flow condition and was, in this regard, uncontrolled.

Model Design

In this work, we have tried to develop an experimental analog to direct numerical simulation calculations whereby we could specify the amplitudes, frequency, and wave angles of disturbances. The approach follows that used in numerous incompressible flows[3,4] with the exception of the actuator. To minimize the required levels of controlled disturbances, the experiment was performed in the 0.5-m Mach 3.5 quiet tunnel at NASA Langley Research Center.

The experimental model we chose was a 7-deg half-angle cone. The model was designed to have a removable tip. For the results presented here, the tip was sharp, with a nose radius of 0.038 mm. The model length was 35.56 cm. For the range of stagnation pressures used in the experiment, the first 30.48 cm (86%) of the model was inside the quiet zone.

A photograph of the cone, three-dimensional traversing mechanism, and support sting is shown in Fig. 1. The cone is of a hollow thin-skin construction. This allowed access to the inside for the placement of thermocouples and pressure ports, as well as wiring for the actuator array. Complete details of the cone construction are given by Cavalieri.[5]

Actuator Array

Our objective was to have actuators that could introduce periodic disturbances that would excite instability modes consisting of pairs of helical waves at the same frequency and equal–opposite wave angles.

Our approach was based on using an azimuthal array of disturbance actuators at one streamwise location.[4] Critical aspects of the design were the azimuthal spacing s of the array elements and the streamwise location of the actuator on the cone. The ideal streamwise position of the actuator is near the location of the lower neutral branch of the linear stability growth curve. The choice of s is based on the range of frequencies and wave angles of the most amplified modes.

Linear stability calculations indicated that the most amplified dimensionless frequencies were in the range from $10 \leq F \times 10^6 \leq 30$, and had wave angles ψ of approximately 60 deg. To maximize the extent of the quiet zone, the experiment was designed to operate at the lowest possible stagnation pressures. We chose P_0 to be 172.35 kPa (25 psi). At this value, and with $T_0 = 311$ K, the actuator location of $x = 14.303$ cm placed it just upstream of the lower neutral branch for the band of most amplified frequencies.

We chose an azimuthal spacing of 15 deg for the individual array elements. Based on this, Table 1 gives the largest wave angles that were possible for the range of frequencies used in the experiment.

The actuator is based on an ac glow discharge. A schematic cutaway drawing of the actuator hub is shown in Fig. 2. The actuator is made up of individual anodes that are supplied with a high-voltage ac signal. The frequency of the ac is that of the instability excitation frequency. The relative phase of the ac controls the instability wave angle. The metal tip of the cone is grounded and, therefore, forms a common cathode. When the voltage is high enough, ionized air (plasma) forms in the cavity. This induces an unsteady jet of fluid that exits through the hole, out of the surface of the cone.

Results

A floating constant-current anemometer was used for making the hot-wire measurements. The concept of the design followed that

Table 1 Excitation conditions based on an azimuthal spacing of 15 deg

f, kHz	$F \times 10^6$	ψ, deg	$n = 2\pi r_{\text{actuator}}/\lambda_\theta$
50	11.9	66	12
60	14.2	62	12
70	16.7	58	12

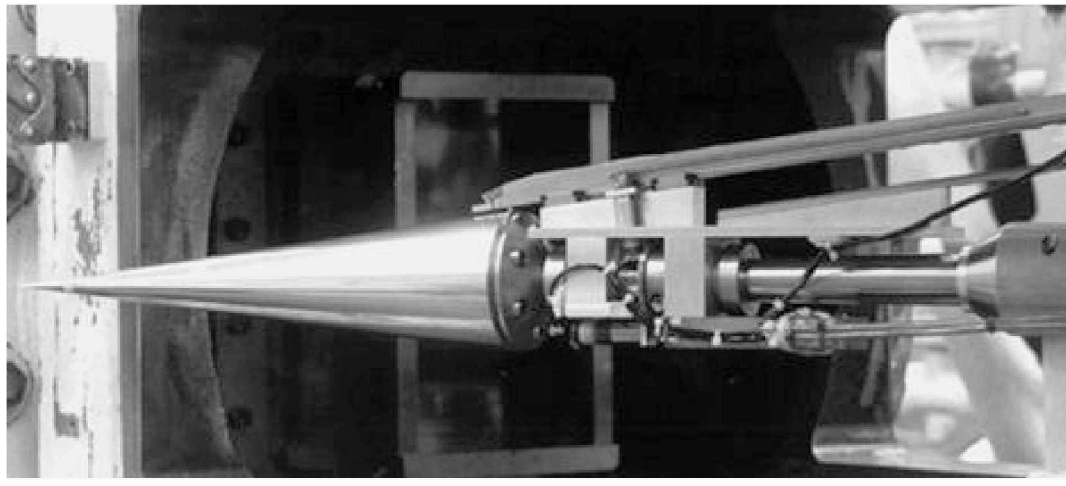

Fig. 1 Photograph of assembled cone, traversing mechanism, and support sting in front of NASA Langley Research Center 0.5-m Mach 3.5 quiet tunnel.

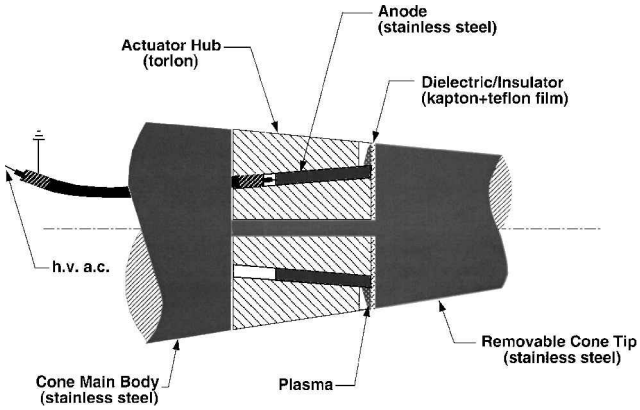

Fig. 2 Schematic cutaway drawing of glow-discharge actuator hub.

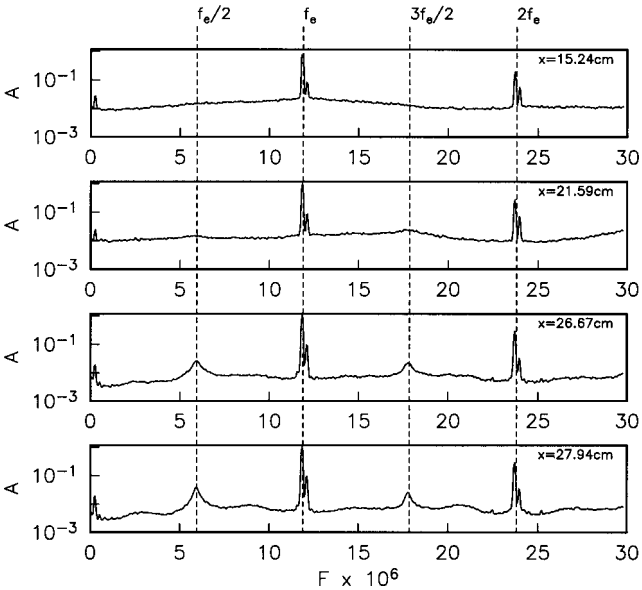

Fig. 3 Spectra at different streamwise locations in the boundary layer, at a fixed height of y = 0.356 mm, with excitation at 50 kHz (F = 11.9 and $\psi = \pm 66$ deg).

described in a private communication by Kendall in 1992 and was found to be necessary when making measurements with the actuator operating. The hot wire was mounted on the traversing mechanism on the model support. In the set of measurements presented here, only a single overheat of 1.7 was used. This overheat was monitored and held fixed as the sensor was moved to different spatial positions. The results are presented in terms of spectra of the anemometer voltage fluctuations. As a result of the high (fixed) overheat, we expect that these are primarily representative of mass-flux fluctuations.

The results presented here are exclusively at an excitation frequency of 50 kHz and $\psi = \pm 66$ deg. Figure 3 shows spectra at a fixed height and different downstream distances from $x = 15.24$ to 27.94 cm. For these, the accuracy in frequency is 122 Hz, which corresponds to $\Delta F \times 10^6 = 0.02$. The peaks at $F = 11.9$ and 23.8 correspond to the excitation frequency f_e and its harmonic, $2f_e$, respectively. The sharp nature of these two peaks suggests that a portion of the hot-wire signal could contain electronic noise from the excitation. Spectra of the control signal (not shown) revealed a similar harmonic, as well as the smaller side peak at the fundamental and harmonic frequencies. However, linear coherence measurements indicated that only the hot-wire fluctuations at the fundamental and harmonic frequencies were phase locked with the excitation signal. Therefore, the other spectral peaks were exclusively a result of the fluid physics and not electronic noise.

The most interesting feature of these spectra is the growth of a subharmonic of the excitation frequency $f_e/2$ at the farther downstream positions. Along with the subharmonic peak, a peak at $3f_e/2$ is also observed. This likely evolves from a summing interaction between the fundamental and subharmonic modes.

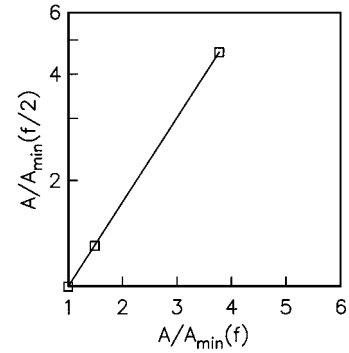

Fig. 4a Response of the subharmonic mode to different fundamental mode amplitudes.

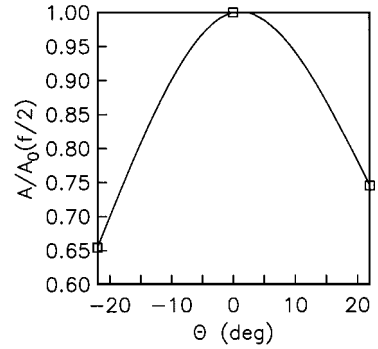

Fig. 4b Subharmonic amplitude azimuthal variation (50-kHz excitation measured at x = 23.5 cm and y = 0.356 mm).

To better understand the origin of the subharmonic, the effect of changing the initial 50-kHz amplitude was investigated. This is shown in Fig. 4a. This was documented at $x = 23.5$ cm, $y = 0.356$ mm, and $\theta = 0$ deg. Here, the initial amplitude above a minimum to produce a plasma was varied by a factor of approximately two. The abscissa corresponds to the measured amplitude at the fundamental frequency normalized by its minimum value. The accuracy of the amplitude is 0.05% of the maximum value.

The ordinate in the plot is the normalized amplitude at the subharmonic frequency on a log axis. If the subharmonic mode results from a secondary interaction with the fundamental, we expect it to have an exponential response to the fundamental mode amplitude. The results seem to support this because the points fall on a straight line on a log axis.

Measurements were taken at different azimuthal positions to determine the azimuthal wavelength of the subharmonic mode. The result is shown in Fig. 4b. This corresponds to the same spatial position as before. The azimuthal angle ranges from ± 25 deg with respect to the 0-deg reference position used in Figs. 3 and 4a. The accuracy in the azimuthal position is 0.56 deg. The subharmonic amplitude has been normalized by the value at $\theta = 0$ deg.

The azimuthal amplitude variation for helical mode pairs should consist of periodic maxima and minima. For the $n = 12$ fundamental mode that was excited, amplitude minima should occur approximately 30 deg apart. A secondary instability analysis in the boundary layer on a flat plate at Mach 1.6 by Ng and Zang,[6] which specified a primary instability of pairs of oblique waves at a fundamental frequency, found the most amplified subharmonic consisted of pairs of oblique waves of comparable wave angles. This appears to be consistent with the spacing of the minima for the subharmonic mode in our experiment.

Conclusions

The experiment to introduce pairs of oblique waves in a supersonic boundary layer on a thin cone revealed the growth of a subharmonic disturbance. The evidence indicates that this corresponds to pairs of oblique waves and that it is due to a secondary instability with the fundamental mode. As such, this is the first experimental observation of this mechanism in this flow. However, more complete experiments that involve documented initial amplitudes and growth rates with calibrated hot-wire sensors are needed to quantify this further.

Acknowledgments

This work was supported by NASA Langley Research Center Grant NCC-1-167 and by Air Force Office of Scientific Research Grant F49620-00-1-0074. The authors are extremely grateful to Steven Wilkinson at NASA Langley Research Center for his unlimited help and expertise in conducting this work. We are also grateful to William Sellers, also at NASA Langley Research Center, for his help in coordinating the use of the NASA tunnels.

References

[1]Kosinov, A., Maslov, A., and Shevelkov, S., "Experiments on the Stability of Supersonic Laminar Boundary Layers," *Journal of Fluid Mechanics*, Vol. 219, 1990, p. 621.

[2]Wilkinson, S. P., Anders, S. G., Chen, F. J., and Beckwith, I. E., "Supersonic and Hypersonic Quiet Tunnel Technology at NASA Langley," AIAA Paper 92-3908, 1992.

[3]Corke, T. C., and Mangano, R. A., "Resonant Growth of Three-Dimensional Modes in Transitioning Blasius Boundary Layers," *Journal of Fluid Mechanics*, Vol. 209, 1989, pp. 93–150.

[4]Corke, T. C., and Kusek, S. M., "Resonance in Axisymmetric Jets with Controlled Helical-Mode Input," *Journal of Fluid Mechanics*, Vol. 249, 1993, pp. 307–336.

[5]Cavalieri, D. A., "On the Experimental Design for Instability Analysis on a Cone at Mach 3.5 and 6 Using a Corona Discharge Perturbation Method," M.S. Thesis, Mechanical and Aerospace Engineering Dept., Illinois Inst. of Technology, Chicago, Aug. 1995.

[6]Ng, L. L., and Zang, T. A., "Secondary Instability Mechanisms in Compressible, Axisymmetric Boundary Layers," AIAA Paper 92-0743, 1992.

J. C. Hermanson
Associate Editor

Influence of Spike Shape at Supersonic Flow Past Blunt-Nosed Bodies: Experimental Study

Snežana S. Milićev* and Miloš D. Pavlović†
University of Belgrade, 11000 Belgrade, Serbia, Yugoslavia

Introduction

BECAUSE of the appearance of a strong shock wave at a supersonic flight of a projectile, which considerably increases the drag and aerodynamic heating during the projectile's flight through the air, a spike is mounted on its nose to reduce this effect.[1–6] In this way, the strong shock wave is replaced with a system of conical waves, so that the driving force, and consequently the fuel consumption, is reduced. A spike mounted on a blunt body during its flight at an angle of attack decreases the drag and also increases the lift. Therefore, all aircraft at supersonic speeds, such as planes, blunt reentry vehicles, rockets, missiles, etc., are usually spike nosed. Even better effects can be attained using such a simple geometrical construction than in the case of sophistically shaped front side of bodies flying supersonically. However, the applicability of the spike is limited due to the possible appearance of oscillations, which may reduce its positive effects and may cause aerodynamics disturbances during the flight.[1–6]

Many researchers focused their attention predominantly on the influence of the spike's length on the aerodynamic characteristics of blunt bodies, for various angles of attack at some transonic,[1] supersonic,[2–5] or even hypersonic[2,6] speeds. However, one might question whether the shape of a spike could affect the fluid flow structure and the aerodynamic characteristics of a blunt body. However, this influence has not been systematically analyzed so far. This Note is a contribution to the study of this effect.

This Note presents the results of an experiment that analyzed the influence of the spike's shape on the drag coefficient and the lift coefficient at supersonic flow past blunt-nosed bodies. The experiment was carried out in a wind tunnel, for one value of Mach and Reynolds numbers and for different angles of attack. The aerodynamic forces for the body without a spike and with four different spike shapes were measured. The Note also proposes a criterion for estimating the aerodynamic effect of the spike shape, by using only the schlieren visualization of the flow. The best spike shape from the experimental set of spikes was selected using this qualitative criterion. This selection coincided with the spike selected by the measurement of the aerodynamic coefficient.

The Note briefly reports the results of the research. An in-depth description of the experiment conditions and results may be found in Ref. 5.

Geometric Characteristics and Experimental Conditions

The geometry of the tested model without and with four different types of spikes[5] is shown in the inset of Fig. 1. The model had a cylindrical body of diameter $d = 27$ mm, with length $L = 4.44d$. Its nose was hemispherical, and its tail was conical, with a semiangle of 9 deg and with a basis diameter $d_b = 0.85d$. All four of the spikes were of the same length $l = d$. The first spike (spike 1) had a cylindrical body with a conical nose with the angle of 20 deg. The second (spike 2) and third (spike 3) spikes were conical with the angles of 5 and 10 deg, respectively. The tips of all of these spikes were rounded. The fourth spike (spike 4) had a hemispherical nose and a cylindrical body. All four spikes, as well as the model, were made of steel and finished with high surface quality.

The experiments were carried out in the wind tunnel T-36 in the Technical Institute of the Yugoslav Army. T-36 is a small trisonic open wind tunnel with interrupted action. The tunnel test section had a cross section 0.25×0.25 m and was 0.6 m long. A classic Teppler system, specially designed to meet high quality and accuracy requirements, was used as the schlieren system for visualization of the fluid flowfield.

The dynamic pressure of undisturbed flow q was taken as the reference value of pressure, the reference area A was the cross-sectional area of the cylindrical body of the model, and the reference

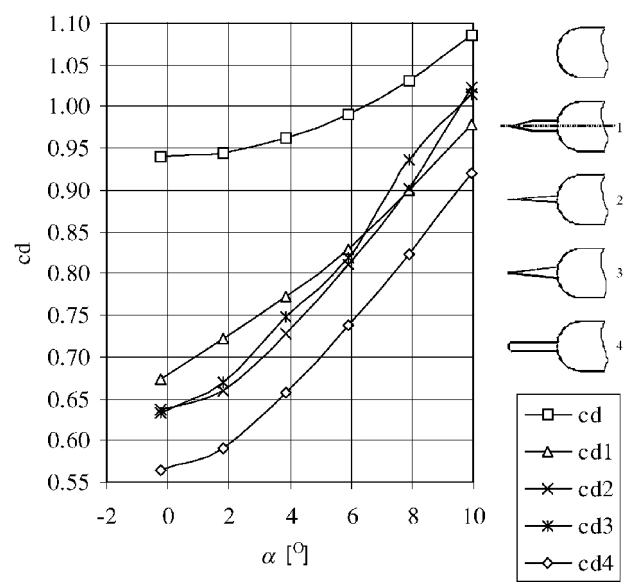

Fig. 1 Relation between the drag coefficient and the angle of attack for the body without (cd) and with the four analyzed spikes (cd1-4).

Received 21 June 2001; revision received 28 January 2002; accepted for publication 29 January 2002.

*Teaching Assistant, Faculty of Mechanical Engineering, 27 marta 80; smilicev@rcub.bg.ac.yu.

†Professor, Faculty of Mechanical Engineering, 27 marta 80.